Deep learning based classification for metastasis of hepatocellular carcinoma with microscopic images

Hui Meng, Yuan Gao, Kun Wang, Jie Tian

Hui Meng, Yuan Gao, Kun Wang, Jie Tian, "Deep learning based classification for metastasis of hepatocellular carcinoma with microscopic images," Proc. SPIE 10949, Medical Imaging 2019: Image Processing, 109492L (15 March 2019); doi: 10.1117/12.2512214

SPIE.

Event: SPIE Medical Imaging, 2019, San Diego, California, United States

Deep learning based classification for metastasis of hepatocellular carcinoma with microscopic images

Hui Meng[a,b], Yuan Gao[a,b], Kun Wang[a,b,c], Jie Tian[a,c,d]
[a]CAS Key Laboratory of Molecular Imaging, Institute of Automation, Beijing, 100190, China;
[b]the University of Chinese Academy of Sciences, Beijing, 100049, China
[c]Beijing Key Laboratory of Molecular Imaging, Beijing, 1000190, China
[d]Beijing Advanced Innovation Center for Big Data-Based Precision Medicine, Beihang University, Beijing, 100191, China

ABSTRACT

Hepatocellular carcinoma (HCC) is the second leading cause of cancer-related death worldwide. The high probability of metastasis makes its prognosis very poor even after potentially curative treatment. Detecting high metastatic HCC will allow for the development of effective approaches to reduce HCC mortality. The mechanism of HCC metastasis has been studied using gene profiling analysis, which indicated that HCC with different metastatic capability was differentiable. However, it is time consuming and complex to analyze gene expression level with conventional method. To distinguish HCC with different metastatic capabilities, we proposed a deep learning based method with microscopic images in animal models. In this study, we adopted convolutional neural networks (CNN) to learn the deep features of microscopic images for classifying each image into low metastatic HCC or high metastatic HCC. We evaluated our proposed classification method on the dataset containing 1920 white-light microscopic images of frozen sections from three tumor-bearing mice injected with HCC-LM3 (high metastasis) tumor cells and another three tumor-bearing mice injected with SMMC-7721(low metastasis) tumor cells. Experimental results show that our method achieved an average accuracy of 0.85. The preliminary study demonstrated that our deep learning method has the potential to be applied to microscopic images for metastasis of HCC classification in animal models.

Keywords: Hepatocellular carcinoma classification, metastasis, microscopic imaging, machine learning, convolutional neural networks (CNN)

1. INTRODUCTION

Hepatocellular carcinoma (HCC) is the sixth most prevalent cancer and the second most frequent cause of cancer-related death.[1] Hepatocarcinogenesis involves multiple steps with accumulation of genetic and epigenetic alternations of the hepatocyte genomes, eventually leading to malignancy development and metastasis.[2] The evaluation of metastatic capability of HCC is an important component of the diagnosis and treatment procedure. Patients with positive metastatic HCC will receive more complex treatment compared with patients negative for metastasis, frequently resulting in more aggressive clinical management.

HCC metastasis is regulated by multiple gene and biomarkers[2-4], which is achieved by liver biopsy. However, it is invasive and limited by sample errors, interobserver variability and various potential complications. Biomarkers, such as enhancer of zeste homolog 2 (EZH2)[2] and N-myc downstream regulated gene 2 (NDRG2)[4], are used to assess HCC metastasis, but their diagnostic performance remains controversial in clinical applications.

Computer-assisted image analysis has been developed to aid in the detection and segmentation of microscopic images. Can et al. achieved accurate classification of colon tissue images based on a deep belief network of restricted Boltzmann machines (RBMs).[5] Authors tested the method on two datasets that contain microscopic images of colon tissues stained with the routinely used hematoxylin-and-eosin technique and obtained accurate classification results. Furthermore, Teramoto et al. developed an automated classification scheme for lung cancers presented in microscopic

*kun.wang@ia.ac.cn; phone 86 82618465-904; fax 86 82618465-904; www.3Dmed.net

Medical Imaging 2019: Image Processing, edited by Elsa D. Angelini, Bennett A. Landman, Proc. of SPIE
Vol. 10949, 109492L · © 2019 SPIE · CCC code: 1605-7422/19/$18 · doi: 10.1117/12.2512214

images using a deep convolutional neural network (DCNN). The developed scheme obtained accurate classification of lung cancers. Recently, Neeru et al. applied a pre-trained Inception-v3 CNN with reverse active learning for the classification of healthy and malignancy breast tissue using optical coherence tomography (OCT) images.[6] The trained network attained accurate classification. However, despite these development, data mining of microscopic images is still under exploration.

Here, we successfully collected two kinds of white-light microscopic images from six tumor tissues, with 1960 microscopic images, which we believe were suitable for the application of the deep learning method. To the best of our knowledge, this is the first prospective study that applied the deep learning on white-light microscopic images for classification of HCC with different metastatic capability. Furthermore, the experimental results demonstrated that our approach can achieve accurate metastasis of HCC classification which can be applied for other applications of cancer research.

2. METHODS

2.1 *In vivo* experiment

Male BALB/c nude mice were purchased from the Beijing Vital River Laboratory Animal Technology Co. Ltd. All animal experiments were performed under the guideline approved by the Institutional Animal Care and Use Committee at Peking University. All animal experiments were performed under isoflurane gas anaesthesia (500 mL/min, Matrx VMR Small Animal Anesthesia Machine, Matrx, USA), and all efforts were made to reduce the pain of the mice. To build the subcutaneous tumor models, 2×10^6 HCC-LM3 (high metastasis) or SMMC-7721 (low metastasis) cells were implanted in the back of mice (n=6). The subcutaneous models were ready for experimentation when tumor volume reached 60 mm^3. After anesthetized with 2% isoflurane, the skin (covering the tumor) was removed and exposed tumor was resected. Following the surgical procedures, the resected tumors were embedded in tissue freezing medium for frozen section.

2.2 Image data acquisition

The frozen sections (10 μm) were taken every 100 μm from each tumor tissue block and imaging with inverted microscope (Leica DMI3000, Germany) equipped with an electron multiplying charge coupled device (EMCCD) camera. Data of microscopic images from each kind of tumor tissue were acquired randomly.

2.3 Image preprocessing

A series of microscopic images (2048 × 2048 × 960) were selected from each kind of tumor. Each image was firstly cut into 512 × 512. Then, the mean stretching was used for enhancement and computation reduction.[7] The mean intensity was computed over an entire image and was used to adjust the intensity of each pixel. The mean intensity is defined as

$$m = \frac{1}{N \times N} \sum_{i=1}^{N} \sum_{j=1}^{N} f(\mathrm{i}, \mathrm{j}), \tag{1}$$

where (i, j) denotes the coordinates of pixel in a given image, f presents the intensity of pixel. N is the dimension of images, which is 512 in our experiment. Mean stretching is implemented based on the following expression.

$$fs(\mathrm{i}, \mathrm{j}) = f(\mathrm{i}, \mathrm{j}) - m, \tag{2}$$

for i=1,2,3,…,N and j=1,2,3,…,N.

2.4 Image classification based on CNNs

In this study, we adopted the CNN method, one of the deep learning techniques, for the automatic analysis of microscopic images. For image classification, microscopic images with the size of 512 × 512 pixels was selected as the input layer, and then the CNN model (Fig. 1) was triggered. Five hidden layers (convolutional layers) were designed in CNN, and each followed with a max pooling layer. Each of the first three hidden layer contained 16 feature maps, and each of the rest two contained 8 feature maps, which were obtained by applying 16 or 8 convolution filters (3 × 3 pixels) to the prior layer. The pooling size was 2 ×2 pixels. At the end, a fully connected layer was applied to connect every neuron in the fifth pooling layer, so that the binary classification can be calculated in the output layer in the form of probabilities.

CNN model was trained based on five-fold cross validation. Four-fifths of the enrolled images were randomly selected as the training cohort, and the rest were used as the validation cohort. Images were sent to the input layer of the CNN model directly, so that the low-level to high-level features included in neural nets' hidden layers were automatically extracted. The model training contains forward computation and back propagation.[8] For forward computation, the input of the CNN model is the microscopic image with a size of 512 × 512. A total of five times of convolution, activation and pooling operations were executed to complete the computation in turn. In our experiments, we adopted the "ReLU" function as activation function, which is defined by

$$\mathrm{ReLU(f)} = \begin{cases} f & f > 0 \\ 0 & f \le 0 \end{cases} \tag{3}$$

When the input is negative, the output of the activation function will be zero, and when the input is positive, the result will be equal to the input. This property helps speed up training process. When it comes to the last fully connected layer and the output layer, the result will be the possibility. For back propagation, we assume the loss function of the whole network is J, and it is defined as following.

$$J(w,b) = \frac{1}{q}\sum_{j=1}^{q}\frac{1}{2}\left[y^j - p_{(w,b)}(x^j) \right]^2 \tag{4}$$

where *j* represents the order of neuron, q is the number of neuron. The most important parameters in the network are the weights w between two neurons and the bias b between two layers. And x is the input of a neuron, $p(x)$ means the actual output of the neuron, while y is the expected output of the neuron. Therefore, J represents the sum of squared error between the actual output and the expected output. In the end, our task is to make J as small as possible, and to achieve this goal, we need to acquire suitable parameters w and b through learning process from data, here we will use gradient descent strategy,[9] which can be defined as follows.

$$w^l := w^l - \alpha \frac{\partial J}{\partial w^l} \tag{5}$$

$$b^l := b^l - \alpha \frac{\partial J}{\partial b^l} \tag{6}$$

where l means the order of the layer, α means the learning rate. The parameters w and b will continue to improve at the end of each iteration of the whole training process. When the loss function tends to decrease and be stable, the CNN model is considered as having completed the training process, which means the CNN model is ready to predict new data.

To quantitative evaluate the performance of classification, sensitivity, specificity and accuracy were used as the quantitative index. Analysis of receiver operating characteristic (ROC) curves was performed to calculate the optimal area under the ROC curve (AUC). The visualization of image classification was further performed using t-SNE (t-distributed Stochastic Neighbour Embedding)[10] and saliency map[11].

Table 1: Quantitative results for tumor classification in five-fold cross validation

Evaluation Index	Validation_1	Validation_2	Validation_3	Validation_4	Validation_5
Specificity	0.80	0.80	0.83	0.88	0.91
Sensitivity	0.83	0.73	0.94	0.83	0.96
Accuracy	0.82	0.77	0.89	0.86	0.93

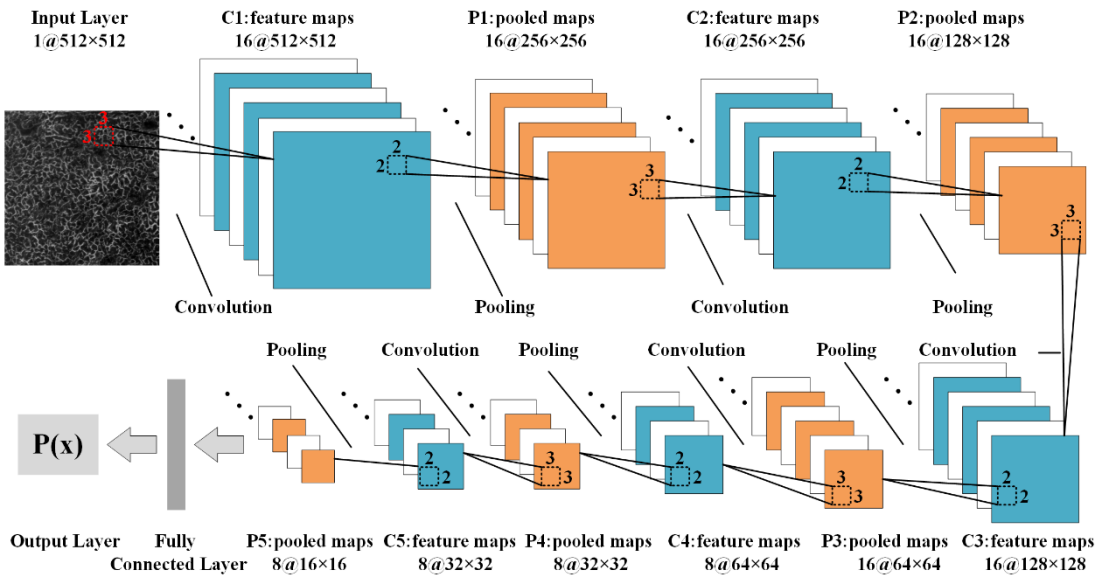

Figure 1: Illustration of the proposed deep learning method for metastasis of HCC classification with microscopic images. An input layer (microscopic image) is analyzed by using five convolution-pooling procedures (C1-P1 to C5-P5), and then last pooled maps are fully connected with 2048 neural nodes to calculate its probability for classification. The neural nodes and other parameters of the convolutional neural network (CNN) model were automatically optimized by using all microscopic images in the training cohorts.

3. RESULTS

AUCs of validation cohorts in five-fold cross validation were 0.89, 0.8, 0.95, 0.92, and 0.96 respectively (Fig. 2(a-e)). Our CNN model obtained an average specificity of 0.84, sensitivity of 0.86, and accuracy of 0.85 (Table 1). From visualization results showed in Fig. 2(f-j), we see clusters of points of the same tumor classes. Furthermore, Fig. 3 presents image-specific class saliency map, highlighting the areas of the given image, discriminative with respect to the given class. Over all, the results demonstrated that deep learning had potential to be used for metastasis of HCC classification based on microscopic images in tumor heterogeneity research.

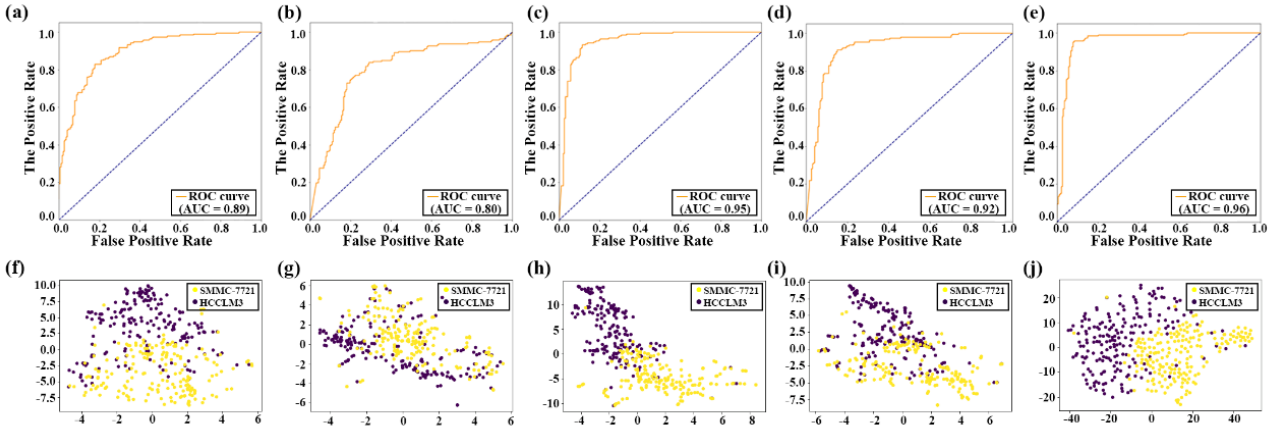

Figure 2: Comparison of ROC curves in five-fold cross validation and t-SNE visualization of the last hidden layer representations in the CNN for hepatocellular carcinoma classification. (a) - (e) show ROC curves of five validation cohorts in five-fold cross validation. (f) - (j) present the CNN's internal representation of two carcinoma classes by applying t-SNE, a method for visualizing high-dimension data, to the last hidden layer representation in the CNN of the five validation cohorts. Purple point clouds and yellow point clouds represent the HCCLM3 and SMMC-7721 tumor, respectively.

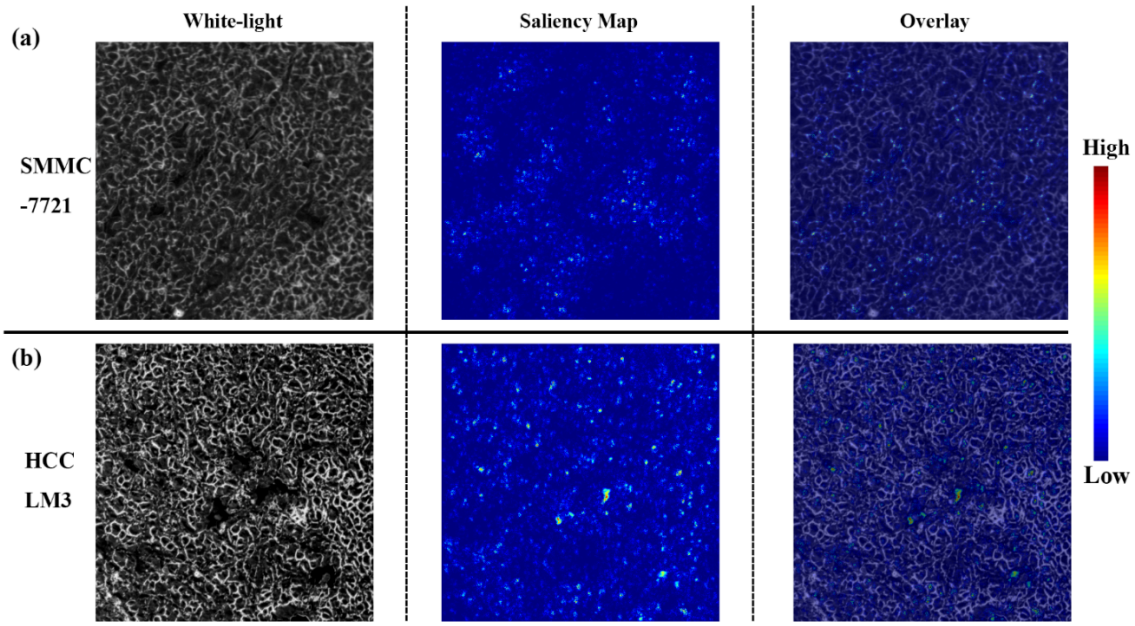

Figure 3: Image-specific class saliency maps for the predicted class in validation cohorts. (a) shows the white-light image (left), saliency map (middle) and the overlay (right) of SMMC-7721 tumor section. (b) presents the white-light image (left), saliency map (middle) and the overlay (right) of HCCLM3 tumor section. The saliency maps were extracted by computing the gradient of the output category with respect to the input to the input image. The high values in the saliency maps indicated that the corresponding pixels present the main features, which are distinguished from the other tumor class.

4. CONCLUSION

In this study, we proposed a deep learning method for metastasis of HCC classification in animal models. The method used CNN to learn the deep features from white-light microscopic images. The proposed method was able to distinguish high metastatic tumor from low metastatic tumor with satisfactory results in this initial experiment. The experimental results demonstrated that our deep learning method is effective for high metastatic HCC detection in animal models. To the best of our knowledge, this is the first prospective study that aimed to achieve metastasis of HCC classification by means of deep learning. It is noteworthy that the classification approach can be extended to other applications of cancer research. The classification results of microscopic images can be combined with biomolecular index, thus the personalized medicine can be developed. Another promising direction is to extend our approach to tumor classification based on microscopic fluorescence images, which can be acquired noninvasively and in real time. All of these suggested a good potential of deep learning for tumor classification. Further studies with more samples are still needed.

ACKNOWLEDGEMENT

The authors would like to thank Yu An, Shixin Jiang, and Lin Yin for the support of *in vivo* experiments. This paper was supported by Ministry of Science and Technology of China under Grant No. 2017YFA0205200, National Natural Science Foundation of China under Grant No. 61671449, 81227901 and 81527805, Chinese Academy of Sciences under Grant No. GJJSTD20170004, XDBS01030200 and QYZDJ-SSW-JSC005.

REFERENCES

[1] Siegel, R. L., Miller, K. D., Jemal, A., "Cancer statistics, 2017," CA: a cancer journal for clinicians 67(1), 7-30 (2017).

[2] Au, S. L., Wong, C. C., Lee, J. M., et al, "Enhancer of zeste homolog 2 epigenetically silences multiple tumor suppressor microRNAs to promote liver cancer metastasis," Hepatology 56(2), 622-31 (2012).

[3] Coulouarn, C., Factor, V. M., Andersen, J. B., Durkin, M. E., Thorgeirsson, S. S., "Loss of miR-122 expression in liver cancer correlates with suppression of the hepatic phenotype and gain of metastatic properties," Oncogene 28(40), 3526-36 (2009).

[4] Lee, D. C., Kang, Y. K., Kim, W. H., et al, "Functional and clinical evidence for NDRG2 as a candidate suppressor of liver cancer metastasis," Cancer research 68(11), 4210 (2008).

[5] Sari, C. T., Gunduz-Demir, C., "Unsupervised Feature Extraction via Deep Learning for Histopathological Classification of Colon Tissue Images," IEEE transactions on medical imaging (2018).

[6] Singla, N., Dubey, K., Srivastava, V., "Automated assessment of breast cancer margin in optical coherence tomography images via pre‐trained convolutional neural network," Journal of biophotonics (2018).

[7] Meng, H., Hui, H., Hu, C., Yang, X., Tian, J., "A fast image registration approach of neural activities in light-sheet fluorescence microscopy images," Proc. SPIE 10137, 1-6 (2017).

[8] Wang, K., Lu, X., Zhou, H., et al, "Deep learning Radiomics of shear wave elastography significantly improved diagnostic performance for assessing liver fibrosis in chronic hepatitis B: a prospective multicentre study," Gut (2018).

[9] LeCun, Y., Bottou, L., Bengio, Y., Haffner, P., "Gradient-based learning applied to document recognition," Proceedings of the IEEE 86(11), 2278-324 (1998).

[10] Maaten, L., Hinton, G., "Visualizing data using t-SNE," Journal of Machine Learning Research 9(2605), 2579-605 (2008).

[11] Simonyan, K., Vedaldi, A., Zisserman, A., "Deep Inside Convolutional Networks: Visualising Image Classification Models and Saliency Maps," Computer Science (2013).